

The KATRIN Neutrino Mass Measurement: Experiment, Status, and Outlook

G. B. FRANKLIN FOR THE KATRIN COLLABORATION¹

*Department of Physics
Carnegie Mellon University, Pittsburgh, PA, 15213*

The Karlsruhe Tritium Neutrino (KATRIN) experiment will provide a measurement of the effective electron-neutrino mass, $m(\nu_e)$, based on a precision measurement of the tritium beta decay spectrum near its endpoint. The effective mass is an average of the neutrino mass eigenvalues m_i weighted by the flavor-mass mixing parameters U_{ei} according to the relation $m^2(\nu_e) = \sum_{i=1}^3 |U_{ei}|^2 m_i^2$. The KATRIN apparatus uses a windowless gaseous tritium source (WGTS) and a spectrometer based on the MAC-E filter concept to measure the beta energy spectrum. The KATRIN program is designed to reach a mass sensitivity of 0.2 eV (90% C.L.). The collaboration has completed a series of commissioning measurements and is moving into the first running of tritium. The KATRIN measurement technique, early commissioning results, and the future outlook will be presented.

PRESENTED AT

The Conference on the Intersections of Particle and Nuclear
Physics
Palm Springs, CA, May 29 - June 3, 2018

¹Primary support for US participation in KATRIN is provided by the U.S. Department of Energy Office of Science, Office of Nuclear Physics, under award number DE-FG02-97ER41020.

1 Introduction

While the bulk of our knowledge of neutrino masses comes from oscillation measurements, oscillation experiments are sensitive to the differences of the squares of the masses and do not determine the absolute neutrino mass scale.

There are several methods for getting at the absolute value of the masses. For example, the spread in arrival time of neutrinos from supernova events has provided insight. Observations of neutrinoless double beta decay could potentially provide information. Neutrino masses may also be observed via kinematic effects; for example, the shape of a beta-decay electron spectrum is sensitive to the neutrino masses. At this time, the absolute mass scale has not been determined and the best upper limits on the neutrino masses from direct measurements give an upper limit of the effective electron-neutrino mass of $m_{\nu_e} < 2$ eV (90% C.L.) [1, 2, 3]. Lower limits have been inferred from the structure in the Cosmic Microwave Background. [4] The KATRIN experiment uses a high precision measurement of the tritium beta decay spectrum for a model-independent determination of m_{ν_e} .

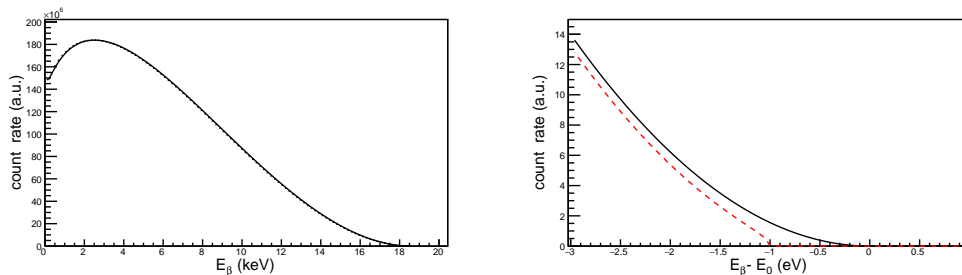


Figure 1: (Left) The ^3H beta-decay spectrum. (Right) The spectrum end-point calculated for two effective neutrino masses, $m_{\nu_e} = 0$ (solid black) and $m_{\nu_e} = 1$ eV. (dashed red)

The calculated energy spectrum of the electrons emitted from the tritium beta-decay, $^3\text{H} \rightarrow ^3\text{He} + e + \bar{\nu}_e$, is shown in Fig. 1a. In principle, the beta-energy endpoint, or maximum electron energy, is determined by the lightest neutrino mass that couples to the beta decay process. The measured spectrum would then have kinks at slightly lower energies corresponding to the kinematic endpoints for each neutrino mass state. However, assuming mass separations much smaller than the experimental energy resolution, the spectrum is only sensitive to an effective electron-neutrino mass, m_{ν_e} defined by averaging the squares of the masses weighted by the mass-eigenvalues to electron-neutrino mixing amplitudes, U_{ej} ,

$$m_{\nu_e} \equiv \sum_j |U_{ej}|^2 m_j^2.$$

Figure 1b shows an expanded view of the spectrum near its endpoint as calculated for two different effective electron neutrino masses, $m_{\nu_e} = 0$ and $m_{\nu_e} = 1$ eV. It can be seen that the spectrum for $m_{\nu_e} = 1$ eV is shifted relative to the $m_{\nu_e} = 0$ and exhibits an altered curvature near its endpoint. Thus a precision measurement of the spectrum shape has the potential to extract the effective electron-neutrino mass, m_{ν_e} .

2 The KATRIN Apparatus

The Karlsruhe Tritium Neutrino experiment, or KATRIN, is sensitive to an effective neutrino mass down to about 0.2 eV.[5, 6] It has two major components: an intense tritium source of beta decay particles and a high resolution integrating spectrometer with better than 1 eV resolution. The electrons from the ${}^3\text{H} \rightarrow {}^3\text{He} + e + \bar{\nu}_e$ decay are detected with a segmented silicon detector, but the eV scale energy resolution is provided by a MAC-E spectrometer. The shape of the spectrum near its endpoint will be used to determine the value of m_{ν_e} .

The layout of the 70 meter long KATRIN apparatus is shown in Fig. 2. On the left, in blue, is the Windowless Gaseous Tritium Source (WGTS). Tritium is pumped in at around 10^{-3} mbar, providing a source of 10^{11} beta decays per second. The beta-decay electrons are transported from the left to the right in the figure; they originate in the WTGS and follow magnetic field lines of a few Tesla through the Main Spectrometer (gray) and then on to the Focal Plane Detector (FPD) located to the right of the Main Spectrometer.

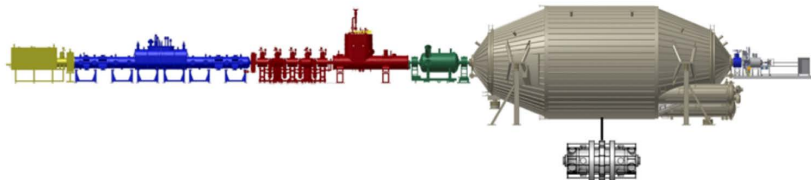


Figure 2: The KATRIN apparatus. The major components are, listing from left to right, the Rear Wall (yellow), the Windowless Gaseous Tritium Source (blue), the differential and cryogenic pumping sections (red), the Pre-Spectrometer (green), the Main Spectrometer (gray), and the section housing the forward focal plane detector section shown on the right.

The required sub-eV resolution prohibits the use of a window between the gaseous tritium source and the spectrometer. In lieu of a window at the exit of the WGTS, a series of differential and cryogenic pumping stations reduce the tritium concentration by 14 orders of magnitude, maintaining an ultra-high vacuum in the main spectrometer vessel that is essentially tritium-free. The Pre-Spectrometer, located just before

the main spectrometer, is set to block all the electrons except the few percent near the beta-spectrum endpoint.

3 The MAC-E Spectrometer

The KATRIN spectrometer achieves its approximately 1 eV electron energy resolution using a MAC-E Spectrometer, a spectrometer based on the concept of a Magnetic Adiabatic Collimator with an Electrostatic Filter.[7] Figure 3 (left photo) shows a view of the MAC-E Spectrometer vacuum vessel as it is being transported to the site of the experiment. The exterior view (center photo) includes some of the air coils that surround the vessel and fine-tune the magnetic field, including compensation for the Earth’s magnetic field. The interior view (right photo) shows vessel’s interior is essentially empty other than electrostatic guard wires near the inner surface used to reflect backgrounds generated in the walls.

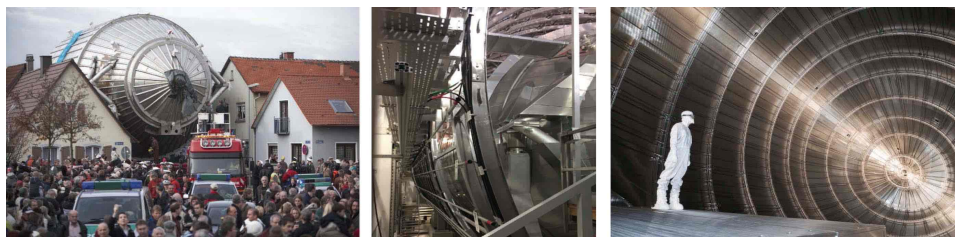


Figure 3: The MAC-E vacuum vessel under transport to the Karlsruhe Institute of Technology and two views (one exterior and one interior) of the spectrometer.

To understand the concept of the MAC-E filter, it is perhaps easiest to first consider the electrostatic potential created by KATRIN’s electrostatic field and initially ignore the magnetic field. Letting z denote the longitudinal position with respect to the spectrometer’s mid-plane, the electrostatic field, $U(z)$, creates a potential energy barrier, $qU(z)$, for the electrons shown schematically in Fig. 4a. The value of the potential barrier at the mid-point is known as the *retarding energy*, qU . As electrons enter the spectrometer, their kinetic energy can be written as a sum of transverse and longitudinal energies. Electrons with a longitudinal energy greater than the electrostatic barrier at mid-point, or *analyzing plane*, cross the analyzing plane and are accelerated back to their original energy as they travel to the exit point of the spectrometer. A post-acceleration region can be used to provide an additional 9 keV of kinetic energy; when this is enabled the electrons originating with energies near the 18.6 keV tritium endpoint reach the detector with about 27 keV of energy and are easily detected in the Focal Plan Detector (FPD) with high efficiency.

The FPD simply counts the number of electrons that reach it. For each potential setting, the count rate, $R(qU_A)$, is a function of the height of the potential energy bar-

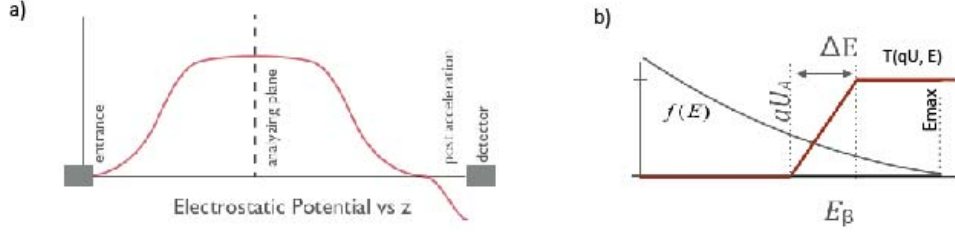


Figure 4: (s) Representation of the electrostatic potential energy barrier $qU(z)$ as a function of position in the MAC-E filter. b) Representations of the transmission function $T(qU, E)$, shown in red, as a function of electron energy for a fixed retarding potential setting qU and beta energy spectrum $f(E_\beta)$ (shown in black) near its endpoint.

rier at the analyzing plane, qU_A . For a fixed retarding energy, the rate is determined by the beta spectrum $f(E_\beta)$, convoluted by the approximately step-like *transmission function*, $T(qU_A, E)$:

$$R(qU_A) = \int_{qU_A}^{E_{max}} T(qU_A, E_\beta) f(E_\beta) dE_\beta.$$

The red line in Fig 4b represents the transmission function and the black line represents the beta energy spectrum, $f(E_\beta)$, near its endpoint. The width of the transition region, ΔE , is the *filter width*. It is determined by the maximum transverse energy of the electrons as they reach the analyzing plane. If one collimated the electrons down to a narrow beam at the source, their kinetic energy would be nearly 100% longitudinal energy, giving an abrupt transition from zero to 100% transmission; ΔE would be very small. Unfortunately, extreme collimation would yield a low count rate and is not practical.

We now consider the functions of the magnetic field constituting the *Magnetic Adiabatic Collimator* part of the MAC-E spectrometer (illustrated in Fig. 5) that provides the mechanism for minimizing the transverse electron energy, and thus the filter width, while maintaining a large angular acceptance in order to obtain high statistics. The electrons follow the field lines, spiraling around them as the magnetic field guides the electrons from the spectrometer's entrance to its exit. Hence the *collimator* part of the MAC-E filter. The 6 T field at the entrance of the spectrometer drops to 3×10^{-4} T at the analyzing plane, a decrease of more than 4 orders of magnitude. The inset in Fig. 5 shows that, as an electron spirals about a field line in a region of decreasing field strength, it experiences a Lorentz force which has a small component along the central field line since the field lines are diverging as the field decreases in magnitude. There is no change in the total kinetic energy, but the transverse kinetic energy is transformed to additional longitudinal kinetic energy.

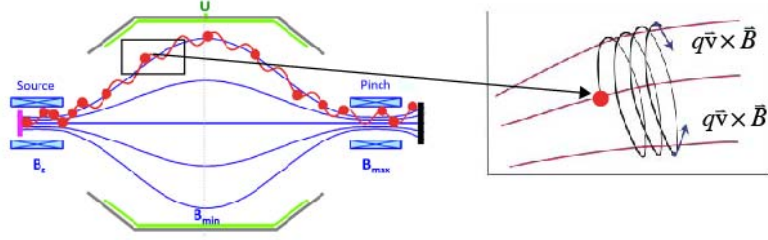


Figure 5: The magnetic field lines within the MAC-E filter. The inset illustrates the cyclotron motion of an electron as it spirals about a field line in a region of diverging field lines results in a component of the Lorentz force along the central field line, resulting in the transformation of transverse kinetic energy to longitudinal kinetic energy.

As an electron follows a field line, the change in field strength is small over one cyclotron orbit and thus the *adiabatic* approximation can be used to easily quantify the transformation of transverse kinetic energy to longitudinal kinetic energy. For this situation, the orbital angular magnetic moment is a constant,

$$\mu = IA = \left(a \frac{v_{\perp}}{2\pi r} \right) (\pi r^2) = \frac{E_{\perp}}{B} = \text{constant}$$

This results in a transverse kinetic energy reduction that is proportional to the reduction in magnetic field. Including a small relativistic effect, the filter width, ΔE , due to the maximum remaining transverse kinetic energy as the electrons reach the analyzing plane can be written as

$$\frac{\Delta E}{E} = \frac{B_A}{B_{max}} \frac{\gamma + 1}{2}$$

The standard KATRIN magnetic configurations of $B_{max}=6$ T and $B_{anal\ plane}=0.3$ mT gives a filter width of 0.93 eV for electrons near the 18.6 keV tritium beta decay endpoint. The complete model of the response function includes effects from inelastic scattering of the betas in the WGTS, Doppler broadening, and modifications to the beta spectrum due to tritium molecular final state binding effects.[8]

The electrons are guided to the Focal Plane Detector by the magnetic field lines. The electrostatic retarding potential at the analyzing plane is actually a function of the radial distance from the axis of symmetry, but the electron's position as it passes through the analyzing plane is mapped to a specific pixel on the detector. We can analyze the data using the appropriate stopping potential value for a given trajectory. The detector's keV-scale energy resolution allows us to put cuts on a region of interest to reduce background events.

The KATRIN apparatus includes a host of additional instrumentation and capabilities used for calibration and monitoring not addressed in this paper, but critical to obtaining reliable results.

4 First Light and Krypton Campaigns

What we call "First Light" was achieved in October, 2016 when electrons, generated through the photoelectric effect on the rear wall, were transported through the entire apparatus and detected in the pixelated focal plane detector. This initial running of the KATRIN spectrometer was used to verify calculations of the flux tube diameter, other system parameters.

KATRIN uses a metastable state of krypton, ^{83m}Kr , as a source of pseudo-mono energetic electrons. This state, shown in Fig. 6a, is created from the decays of Rubidium and has a half-life of 1.83 h; it can be used within the apparatus with no long-term contributions to backgrounds. The metastable state decays through two successive electron conversions. Figure 6b, shows that the first 32.1 keV nuclear de-excitation results in the ejection of a conversion electron whose energy depends on the initial atomic shell of the electron. This process results a series of pseudo mono-energetic electron lines denoted K-32, L-32, M-32, etc. with the energies shown in the figure. The subsequent nuclear de-excitation from the 9.4 keV nuclear level also occurs through electron conversion, resulting in a second series of ejected electron energies labeled L-9.4, M-9.4, etc. (The 9.4 keV nuclear de-excitation does not provide sufficient energy to eject a K-shell electron.) The KATRIN spectrometer's sub-eV resolution is actually sensitive to the initial atomic sub-shell energy splittings, so the complete conversion electron labeling convention includes the sub-shell. For example, L2-32 notation denotes the a 32.1 keV nuclear de-excitation ejecting an electron from the second sub-shell of the L-shell atomic krypton atom.

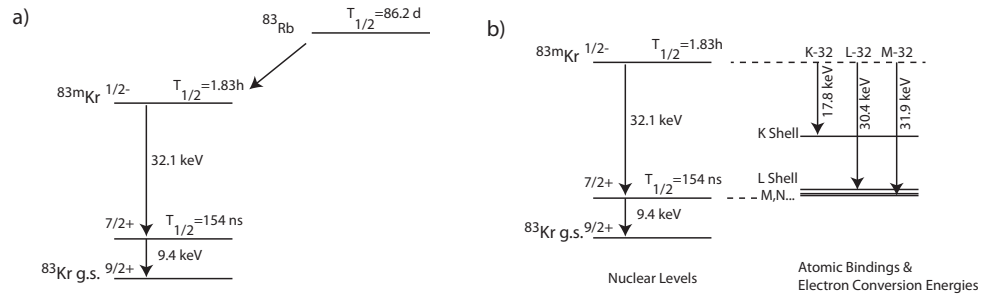


Figure 6: a) The relevant energy levels of the ^{83}Kr nuclear energy levels fed from the beta decay of ^{83}Rb . b) The ^{83}Kr electron shell levels and the corresponding electron conversion energies associated with the nuclear 32.1 keV de-excitation.

The KATRIN apparatus includes two krypton sources within the apparatus in

addition to one used in the HV monitoring spectrometer. A small condensed krypton source can be inserted and moved about to test the mapping of source location within the flux tube to specific pixels in the Focal Plane Detector. In addition, gaseous krypton can be injected into the WGTS to generate a homogenous distribution in the detector. This can be done while maintaining tritium in the WGTS and allows measurements of the transmission function, including effects due to the electrons interacting with the tritium gas.

Figure 7 shows the results from a gaseous krypton run performed in the summer of 2017. In Fig. 7a, the data points (blue) show the measured FPD counting rates as the retarding energy is stepped through a series of energies, sweeping through the energy corresponding to the krypton L3-32 electron conversion line. The pseudo-monoenergetic conversion electron data are modeled with three parameters: line position, width, and amplitude and a fourth parameter is used to allow a flat background under the conversion electron peak. This 4-parameter characterization is then folded with the calculated KATRIN response function and fit to the data. The resulting fit is shown as the orange curve and the corresponding line shape, given by these four fitted parameters, is shown as the dashed green line in Fig. 7a. Figure 7b shows similar results for a scan over the K-32 line energy. The stability of the KATRIN spectrometer is demonstrated in Fig. 7c, which shows the variation in the fitted line position as a function of time over five days of running. This demonstrated stability is well within the KATRIN design limit of $\pm 60\text{meV}$ as shown in the figure.

As of the date of this conference, KATRIN has published two papers on the *First Light* and *Krypton* campaigns and a half-dozen more are undergoing the KATRIN Collaboration review process.[9][10]

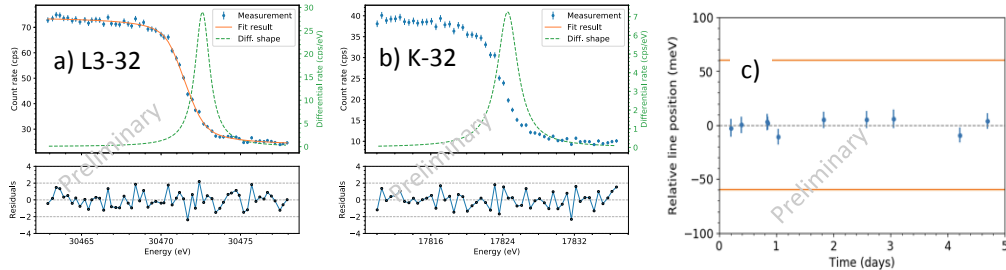


Figure 7: Results from the first gaseous krypton measurements. a) The FPD count rate as a function of retarding energy setting shown as blue data points. The orange curve is a 4-parameter fit to the data and the green curve is the corresponding extracted L3-32 line shape. b) Similar for a scan over the K-32 line position. c) The relative extracted line position as a function of time.

5 Status and Outlook

The very first tritium was injected into the WGTS on May 18, 2018, only a few weeks before this conference. Initial ion-safety and sub-system check outs were performed using a D₂ carrier gas with 1% tritium. The first tritium beta-decay energy spectra were measured the following day. At this time, the commissioning is continuing with the first low-concentration tritium running and the initial results are being prepared for the *Neutrino 2018* conference. Over the next year, we expect to make additional commissioning and krypton measurements and then proceed to acquire the initial tritium datasets. We expect to initiate a search for kinks in the beta spectrum that could signify the existence of a sterile neutrino in the keV mass range. This search could be *Phase 0* of a program being developed to search for signatures of sterile neutrinos.

ACKNOWLEDGEMENTS

I am grateful for the opportunity to present the work of the entire KATRIN contribution and, in particular, the contributions of Larisa Thorne and Prof. Diana Parno to the preparation of this talk. The KATRIN collaboration acknowledges the support of Helmholtz Association (HGF), Ministry for Education and Research BMBF (05A17PM3, 05A17PX3, 05A17VK2, and 05A17WO3), Helmholtz Alliance for Astroparticle Physics (HAP), and Helmholtz Young Investigator Group (VH-NG-1055) in Germany; Ministry of Education, Youth and Sport (canam-lm2011019), cooperation with the JINR Dubna (3+3 grants) 20172019 in the Czech Republic; and the Department of Energy through grants DE-FG02-97ER41020, DE-FG02-94ER40818, de-sc0004036, DE-FG02-97ER41033, DE-FG02-97ER41041, DE-AC02-05CH11231, de-sc0011091 and de-sc0019304 in the United States.

References

- [1] C. Kraus, *et al.*, Eur. Phys. J., **C40**(4), 447 (2005).
- [2] V.N. Aseev, *et al.*, Phys. of Atomic Nuc. **75**, 446 (2012).
- [3] K.A. Olive, *et al.*, Chin. Phys. **C38**, 090001 (2014).
- [4] F. Couchot, *et al.*, Astron. Astrophys. **606** A104 (2017).
- [5] J. Angrik, *et al.*, <http://inspirehep.net/record/680949/files/FZKA7090.pdf>
- [6] J.F.Amsbaugh, *et al.*, Nucl. Instrum. Meth. **A788** 40-60 (2015).

- [7] G. Beamson, H. Porter, & G. Dturner, J. Phys. E Sci. Instrum. **13** 64 (1980).
- [8] M. Kleesick, *et al.*, Eur. Phys. J. C to be published, arXiv:1806.08312 (2018).
- [9] M. Arenz, *et al.*, JINST **13** 04020 (2018).
- [10] M. Arenz, *et al.*, Eur. Phys. J., **C78**, 368 (2018).